Journal of Applied Electrochemistry **32**: 1043–1048, 2002.

An *in situ* spectroelectrochemical Raman investigation of Au electrodeposition and electrodissolution in $KAu(CN)_2$ solution

B. BOZZINI* and A. FANIGLIULO
INFM – Dipartimento di Ingegneria dell'Innovazione, Università di Lecce, v. Monteroni, I-73100 Lecce, Italy
*(*author for correspondence, fax: +39 0832 320525, e-mail: benedetto.bozzini@unile.it)*

Received 13 November 2001; accepted in revised form 23 April 2002

Key words: cyanoaurate, electrodeposition, electrodissolution, gold, Raman

Abstract

Spectroelectrochemical behaviour of CN^- on a Au electrode in a $KAu(CN)_2$ bath at pH 6.3 was studied by *in situ* confocal Raman spectroscopy. Internal (CN stretch) and external (Au–CN) CN^--related frequencies were investigated under potentiostatic control in a potential interval spanning cathodic and anodic ranges (−1800 to +1200 mV vs Ag/AgCl). Electrochemical behaviour was assessed by cyclic voltammetry. Stark-shifted Au–NC^- species are the dominating ones under cathodic polarization. Above the hydrogen evolution potential a Au–H stretch band can also be observed. At open circuit Au–CN^- species tend to prevail, while anodic conditions relate to the enhanced formation of $Au(CN)_2^-$ and OCN^-.

1. Introduction

A large corpus of spectroelectrochemical data is available for adsorbed CN^- onto Ag and Pt. CN^- is typically adsorbed from KCN or NaCN solutions as a function of applied potential by two approaches: (i) directly in the spectroelectrochemical cell, (ii) in a separate cell; the adsorbed layer is later transferred into a different electrolyte where it is studied spectroelectrochemically. Much less work has been carried out on the Au/CN^- system; in the few papers available CN^- adsorption was carried out from alkaline KCN solutions. Spectroelectrochemical work on CN^- adsorption onto polycrystalline Au based on SERS [1–3] and IR [2, 4–6] mainly points towards a fundamental understanding of the behaviour of the ν(CN) stretch band. This band is located at about 2100 cm^{-1} and displays the following Stark shift values in the open-circuit to cathodic range (−1200 to −500 mV vs Ag/AgCl): 12 cm^{-1} V^{-1} by SERS [3], and 33 cm^{-1} V^{-1} by FTIR [7]. Early polarization-modulated FTIR-RAS work assigned the ν(CN) stretch band at about 2100 cm^{-1} to linearly adsorbed CN^- [6] and $Au(CN)_2^-$ as a function of operating conditions. Recent theoretical work based on quantum chemical methods [8] discusses the ν(CN) Raman shift values for Au–CN^- and Au–NC^- bonding. Potential-dependent IR and SERS ν(CN) spectra for the Au/CN^- system were compared in [2] and proved to yield very similar results, as more recently shown in detail for the Pt/CN^- system. From the literature it can be concluded that the nature of the surface cyanide species and electroactive intermediates giving rise to SERS are still not fully known and are strongly dependent on the experimental conditions.

The behaviour of the system in the low-frequency range (~300 to 400 cm^{-1}) was dealt with in [3, 9]. Several bands were observed in this range, the assignment of which is not unambiguous. It is worth stressing that this complexity is also a feature of the vibrational spectra of pure crystalline metal cyanocomplexes [10]. Work on the spectroelectrochemical behaviour of cyanide-containing species other than free CN^- (and in particular on electroactive metal cyanocomplexes) is not available, to the best of the authors' knowledge.

A limited amount of work by *in situ* spectroelectrochemical methods was carried out during the course of electrodeposition [11–14]; apart from [13], these papers deal with adsorbed CN^- bands. No spectroelectrochemical work is available – as far as the authors are aware – on the electrodeposition of Au from the $Au(CN)_2^-$ complex. Molecular level understanding of this system is very critical for the improvement of the plating systems for the following reasons: (i) avoidance of deposit brittleness, (ii) elimination/substitution of the toxic and polluting additives traditionally employed in the plating practice, (iii) management of low-Au-concentration baths. In this paper we focus on the CN^--related bands in the low (~200–500 cm^{-1}) and high-frequency (~2100 cm^{-1}) ranges with the aim of elucidating the nature of the surface species and its bearing on the electrodeposition process. In the literature, most attention has been devoted on the vibrational frequency shifts of internal adsorbate modes upon surface binding, the frequencies of the surface-adsorbate modes themselves

are of potential significance for the understanding of metal-electroplating phenomena. Apart from specific interest for electroplating, the present work also extends the fundamental knowledge of the Au/CN^- system in that: (i) it studies the CN^- adsorption behaviour in a metal–cyanocomplex solution; (ii) it extends spectral work to the low-frequency range, where metal–adsorbate vibrations are active; (iii) it deals with a near-neutral solution (pH 6.3).

It is worth observing that the controversy about the fact that the SERS signal derives from peculiar sites or, on the contrary, it gives a sufficiently average information on adsorbed species, is still not settled. In general it could be expected that IR detects the majority species, while SERS may only detect a fraction of species adsorbed at SERS-active sites. This matter is particularly relevant to electrodeposition problems where site-specificity could be, in principle, either an advantage (high sensitivity to morphology development) or a drawback (possibly unreliable information on the degree of surface coverage or coadsorption). The literature is not unanimous, conclusions of reports comparing Raman and IR work on CN^- adsorption range from the assessment of marked diversity of results [7] to extreme similarity [2]. Relevant work is in progress in our group, oriented to metal-plating problems.

2. Experimental details

The Au bath was: $KAu(CN)_2$ 10 g l^{-1}, citric acid 40 g l^{-1}, ammonium citrate 40 g l^{-1}, pH 6.3 (KOH and citric acid), 25 °C.

Electrochemical measurements were carried out in a H cell containing 0.2 dm^3 of bath. Cathodic and anodic compartments were separated by a glass frit. The working electrode (WE) was Au wire. The WE was ground with 1200 grit SiC paper and sonicated in distilled water before each experiment. The counter electrode (CE) was Pt wire. The reference electrode (RE) was Ag/AgCl. Voltages are reported vs Ag/AgCl. Cyclic voltammetry (CV) measurements were carried out in a solution with the same citrate concentration, but with $KAu(CN)_2$ 1 g l^{-1}, at a scan rate of 20 mV s^{-1}.

SERS measurements were carried out with a Raman microprobe system (LabRam Jobin–Yvon) equipped with a confocal microscope, CCD detector, holographic notch filter and mapping facilities with micrometric lateral resolution. Excitation at 632.8 nm is provided by a He–Ne laser and the power delivered at the sample was about 12 mW. A 10× long-working-distance objective was used. *In situ* electrochemical measurements were performed in a Ventacon cell with a vertical polycrystalline Au disc WE of diameter 3 mm embedded into a Teflon holder. Metallographic polishing with 1200 grit paper before each experimental run, mentioned above, proved adequate for excellent reproducibility of spectroelectrochemical measurements. The CE was Pt wire and the RE Ag/AgCl.

The acquisition time was varied in the range 20–800 s in order to maximise the signal-to-noise ratio, compatibly with possible disturbances arising from high rates of electrodic reaction (high cathodic and anodic ranges), typical values are around 250 but significantly lower figures where achieved at high cathodic and anodic voltages. Background subtraction was performed by means of a 7th order polynomial interpolation curve. Data analysis was carried out by interpolation with gaussian curves (for the limits in the use of a gaussian band shape (e.g., [15]). The nonlinear optimisation of the fitting parameters was carried out by the maximum gradient iterative method. Stopping criteria were either maximum relative variation of parameter estimate of 0.001 or computation time of 300 s.

3. Results and discussion

3.1. *Cyclic voltammetry*

Cyclic voltammograms (CV) in the ranges −1800 to +1200 mV and −1400 to −400 mV were recorded for the investigated electrodeposition bath (Figures 1 and 2). A report on the behaviour of citrate on Au electrodes in solutions not containing $KAu(CN)_2$ will be prepared separately, just some facts will anticipated here. (i) Citrate is not oxidized at Au in the investigated anodic range. (ii) Presence of citrates in solution suppresses hydrogen-oxidation features in the anodic range of the return scan after the cathodic Tafel region, probably owing to adsorption of citrate-related species. This suppression is expected to be further enhanced by CN^- adsorption, as reported for Pt in both alkaline [16] and neutral [17] solutions. (iii) Hydrogen evolution from the carboxylic groups of citrate can take place. (iv) Au oxidation occurs at potentials more anodic than about +400 mV and three peaks related to Au reduction can be noticed at about +300, −400 and −800 mV. Addition of $KAu(CN)_2$ brings about the following changes. Au-oxidation seems to be enhanced, probably owing to

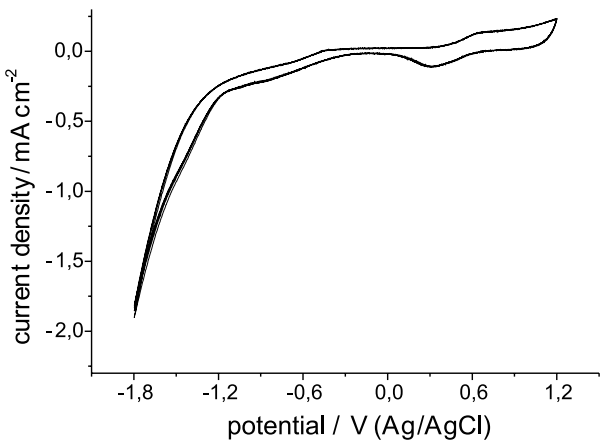

Fig. 1. Cyclic voltammogram for Au electrodeposition bath. Scan rate 20 mV s^{-1}.

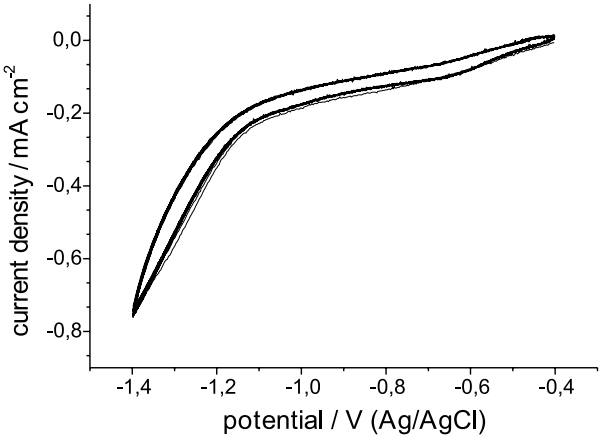

Fig. 2. Cyclic voltammogram for Au electrodeposition bath. Scan rate 20 mV s^{-1}.

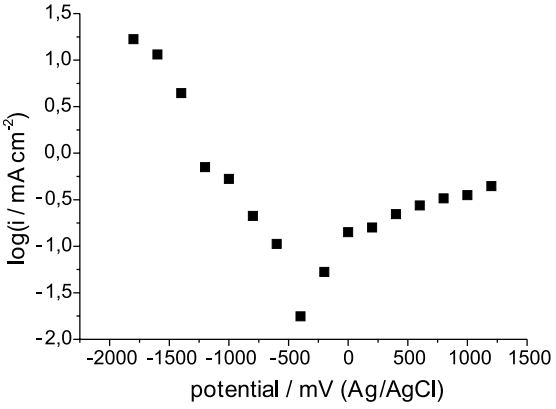

Fig. 3. Steady-state current density values recorded during potantiostatic polarization and *in situ* spectroelectrochemical measurements.

the CN^--containing environment (some free-CN^- is released during the cathodic scan). A dominating reduction peak can be obtained from anodically oxidised Au at a potential slightly more cathodic than in the absence of the Au(I) salt. Au reduction from $Au(CN)_2^-$ occurs at about −750 mV and the respective reoxidation peak can be observed at about −650 mV [7, 18]. An evolution of CVs towards an asymptotic cycle can be observed. In the first few cycles higher currents can be recorded at a given voltage, which tend to decrease with time. Progressive inhibition, reasonably through release of CN^--related species, can be noticed. The time-dependent behaviour of the polarization needed to achieve a current density (c.d.) level of 1.0 and 1.75 mA cm^{-2} can be approximated with a single exponential decay with a time-constant of 2.3 ± 0.2 s. A shoulder appears at $V < -1100$ mV, related to Au electrodeposition, followed by a Tafel-type growth, linked to simultaneous Au electrodeposition and hydrogen evolution.

Figure 3 illustrates the steady-state potentiostatic polarization curve recorded during spectroelectrochemical measurements. Steady-state c.d. values are typically reached 100 s after applying the potential step from open-circuit conditions. Recording of spectra is started 180 s after application of the potential. The cathodic region starts at about −400 mV. A cathodic quasi-Tafel behaviour can be observed with an apparent slope of about 500 mV dec^{-1}, which has been interpreted in terms of a C–E mechanism with a decomplexing chemical rate determining step [19]. At potentials more negative than −1200 mV H_2 gas is visibly evolved. This phenomenon can be correlated with the limiting-current related drop observed around −1200 mV, logarithmic growth resumes for higher cathodic potentials because of hydrogen-evolution related electrolyte stirring. At anodic potentials, very low c.d.s are recorded, the surface being probably passivated by hydrous Au(III) oxide films, beginning to form around +400 mV (see also [20]).

3.2. *Spectroelectrochemical measurements*

3.2.1. *ν(CN) stretch band*

In situ Raman spectra relative to steady-state (as far as peak position and shape and c.d. are concerned) achieved at different anodic and cathodic voltages (−1800 to +1200 mV) are shown in Figures 4–6. In the whole set of experiments, five kinds of peaks could be noticed, their phenomenological characteristics are reported in Table 1. Peak heights are not reported in this paper because they depend in a very informative, though complicated, way on instantaneous potential-dependent cathode roughness; a specific report relating roughness produced by electrodeposition to surface Raman enhancement for the relevant bands will be produced. At mildly cathodic potentials (∼−1200 to −800 mV) the Stark-shifted type I band around 2100 cm^{-1} dominates. Two different Stark-shift values are measured in the potential range in which no significant hydrogen evolution occurs (48 ± 2 cm^{-1} V^{-1}, $\rho^2 = 0.99$, Figure 7) and in the one in which hydrogen evolution visibly occurs (20 ± 4 cm^{-1} V^{-1}, $\rho^2 = 0.93$, Figure 7). At higher

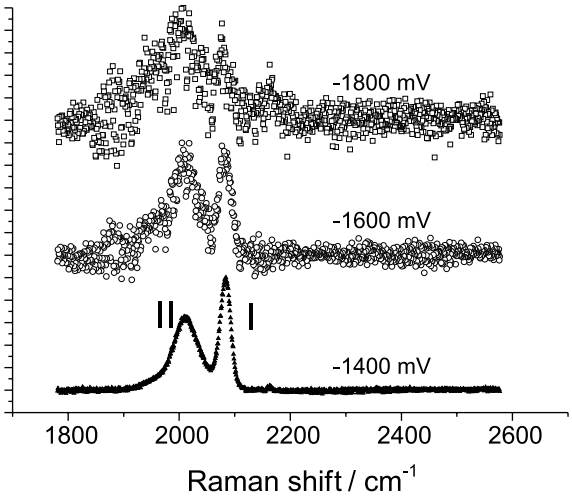

Fig. 4. Raman spectra of the CN^- stretch band as a function of applied potential from −1800 to −1400 mV vs Ag/AgCl.

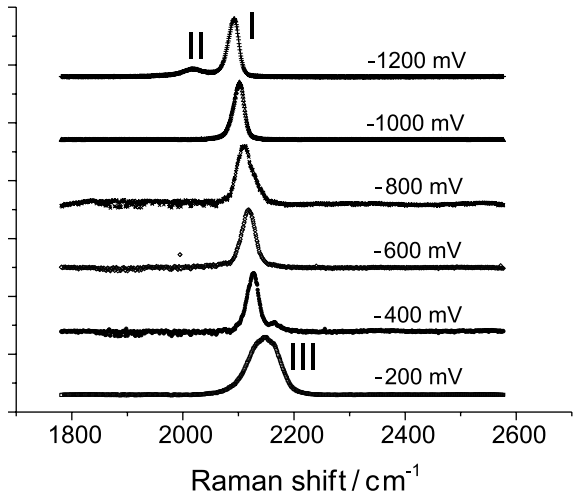

Fig. 5. Raman spectra of the CN^- stretch and Au–H bands as a function of applied potential from −1200 to −200 mV vs Ag/AgCl.

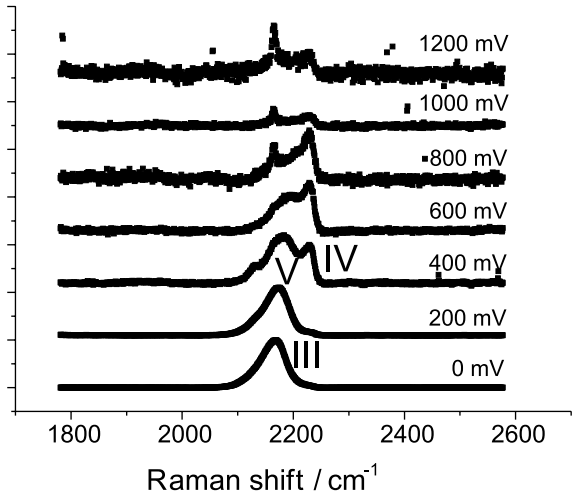

Fig. 6. Raman spectra in the CN^- stretch range as a function of applied potential over the range 0–1200 mV vs Ag/AgCl.

cathodic potentials (∼−1800 to −1200 mV) one further Stark-shifted band II appears at about 2000 cm^{-1} (35 ± 4 cm^{-1} V^{-1}, $\rho^2 = 0.98$, Figure 7) and tends to dominate over band I as the potential grows cathodic. As potentials grow more positive than −400 mV a Stark-shifted type III band appears at around 2150 cm^{-1} (39 ± 5 cm^{-1} V^{-1}, $\rho^2 = 0.90$, Figure 7) and grows in relative intensity in the range from −400 to +400 mV. For potentials more positive than 0 V, the type IV band

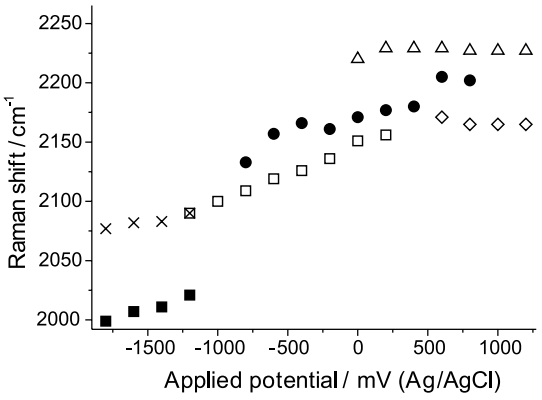

Fig. 7. CN stretch band positions (from gaussian fits) as a function of potentiostatic polarization conditions. Key: (□) Au–NC, (■) Au–H, (●) Au–CN, (△) Au–CNO, (◇) $Au(CN)_2^-$ and (×) Au–NC, H-evol. range.

around 2250 cm^{-1} appears. The peak position for this band does not depend appreciably on applied cathode potential. At strongly anodic potentials bands III and IV tend to disappear, while type V band around 2150 cm^{-1}, whose peak position is not a function of applied potential, tends to be stabilised. Full width at half maximum (FWHM) of the fitted bands is consistent with typical literature values, this kind of bands is rather broad, probably owing to the details of the surface structure [21]. More comments concerning FWHM of the type II band will be reported in the following.

In accord with literature experimental data on cognate systems and theoretical analyses, bands I and III can be interpreted in terms of CN^- stretch, bound to Au through N and C, respectively. [22] reports SFG experiments on Pt showing Pt–CN^- (at 2150 cm^{-1}) and Pt–NC^- (at 2070 cm^{-1}) species, such species have further been proved to be simultaneously present at from $V = -600$ to 200 mV, irrespective of surface structure and crystallinity [17]. Computations based on quantum mechanical approaches predict Raman shifts for ν(CN) related to Au–CN^- and Au–NC^- which are compatible with our data [8]. The difference in orientations is essentially due to electrostatic charging of the cathode, stabilising the N-bound configuration, with respect to the C-bound one under electrodeposition conditions. Literature observations concerning partial charge transfer to the electrode in the formation of Au/CN^- adsorbed complexes [1] is compatible with reorientation behaviour. Reduction of type I peak intensity

Table 1. Phenomenological characteristics of CN stretch bands observed as a function of potential (peak positions and FWHM by gaussian fit)

Band designation	Raman-shift range /cm^{-1}	Stark-shift /cm^{-1} V^{-1}	FWHM /cm^{-1}	Potential range /mV	Tentative band assignment
I	2077–2156	48 ± 2, no H↑ 20 ± 4, H↑	14–26	−1800 to +200	Au–NC^-
II	1999–2021	35 ± 4	42–88	−1800 to −1200	Au–H
III	2133–2205	39 ± 5	18–52	−400 to +800	Au–CN^-
IV	2217–2229	≅0	16–24	0 to +1200	Au–CNO^-
V	2165–2171	≅0	7–19	+200 to +1200	$Au(CN)_2^-$

at the highest cathodic voltages might be related to electrostatic CN^- desorption. For a range of potentials higher than the open-circuit one, both bands coexist, this might be, at least in part, due to the sluggishness of CN^- reorientation processes [23] and to the presence of electroactive Au(I) cyanocomplexes. Similar results were not reported in the literature, which (as detailed in Section 1) invariably deals with CN^- adsorbed from alkaline-earth solutions.

In principle, the adsorbed CN^- species, at the pH of this experiment, could be hydrated. In [16] a IR band is reported at 2147 cm^{-1} regarding a surface cyanide layer on Pt in which CNH is the predominant species at pH 8. In [24] potential dependent ν(CN) spectra are shown at about 2250 cm^{-1} explained with Pt–CNH species and contrasted with Pt–CN^- at about 2200 cm^{-1}. The M–CN^- $\leftrightarrow$ M–CNH transition is reported to be rapid and reversible [16] while that of M–CN^- $\leftrightarrow$ M–NC^- is expected to be sluggish, owing to bond-breaking, adsorbate reorientation and subsequent bonding processes. These observations, complemented by our kinetic data reported in [23], give support to the interpretation of type I band as Au–NC^- and type III as Au–CN^-, irrespective of the possibility that both, or the latter, of these species be hydrogenated.

Significant differences in Stark shift values are observed in our spectra with respect to values in the literature (Section 1). The observed higher values might be explained with peculiarities linked to lateral interaction of CN^- related to the $Au(CN)_2^-$ complexes or coadsorbed citrate or atomic hydrogen.

Concerning the type II band, both polarization conditions and reference to cognate literature for Pt electrodes [25–29] suggest the interpretation of this peak as linked to Au–H stretch. In [25] SERS work is reported on Pt electrodes in the hydrogen evolution range of potentials for pH 0–14. A wide band ($\sim$70–90 cm^{-1}) centred in the range 2039–2094 cm^{-1} (position and width depend on the pH) was observed and related to Pt–H stretch due to singly-coordinated H on top of a surface metal adatom [26]. Similar, though less explicit, results concerning the Pt/H adsorption system were reported by SFG [28, 29] and IRAS [27]. Observation of a further peak at 1646 cm^{-1} in [25] was associated with δ(H-O-H) of bulk water, this band was not observed in our work, probably because the confocal volume in our instrument is $\sim$0.2 μm^3 against $\sim$9 μm^3 of [25] thus allowing more efficient rejection of bulk electrolyte signal. The marked width of the ν(Pt–H) reported in [25] is similar to that we measured for the ν(Au–H) (42–88 cm^{-1}); both can be explained on the basis of homogeneous band broadening.

Peak IV is very similar to that measured by IR for OCN^- adsorbed onto Pt [30] at 2170 cm^{-1}. The observed intensity decrease with increase of anodic potential supports this explanation. The appearance of some structure in the spectra at about 2350 cm^{-1} is compatible with CO_2 formation under oxidizing conditions, [16]. The fact that the peak position of band IV is not affected by the applied potential, even though it is most reliably related to surface species [16] can be explained with the fact that this surface species is not significantly charge-coupled with the metallic surface.

Band type V can be related to $Au(CN)_2^-$ species, observed at 2146 cm^{-1} on anodically polarized Au [7]. Unpublished Raman spectra recorded in our laboratory for crystalline $KAu(CN)_2$ show that the ν(CN) band is located at 2154 cm^{-1}. Comparison of p- and s-polarized IR spectra [7] proved that this oxidation product is indeed present at the surface, a different species is observed in the bulk. Both the data of [7] and ours show that the peak position is not affected by the applied potential. The absence of a Stark shift with these surface species can be explained, as for OCN^-.

3.2.2. *Low-frequency vibrations involving species bonded to Au*

Polarized Au electrodes give rise to reproducible peak structures, shown in Figure 8. In the investigated anodic range (+600 to +1200 mV) the potentials are too low for citrate oxidation. A strong potential-dependent band dominates in the range 500 to 600 cm^{-1} the variation is probably too large to be due to Stark shift and can be tentatively related to the formation of Au(I) species which are progressively more loosely bound to the surface, as anodic conditions prevail and dissolution is favoured. Minor – not easily resolvable – features might be related to adsorbed OCN^- species.

In the investigated cathodic range (−1800 to −600 mV) the polarization tends to enhance the peaks C, D, E and F and to depress peaks A, B. Bands A and B are at Raman shifts close to those mentioned by [3] at about 300 and 380 cm^{-1} and assigned to ν(Au–C) and δ(Au–CN). These authors did not go into details concerning CN^- orientation with respect to the Au surface and their interpretation is not incompatible with our own of bands at about 2100 cm^{-1} implying Au–N

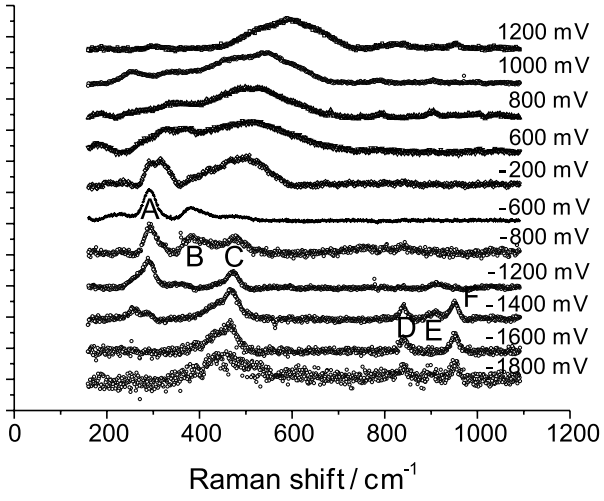

Fig. 8. Raman spectra in the frequency range typical for vibrations of Au-bonded species as a function of applied potential from −1800 to 1200 mV vs Ag/AgCl.

bonding under electrodeposition conditions. The spectra at −200 mV, displaying a wide band at about 500 cm^{-1}, as well as lower intensity for bands A and B, can be well interpreted as related to Au-C vibrations, compatible with our previous discussion of ν(CN). The quantum computations of [8] for ν(Au–C) and ν(Au–N) give support to our interpretation. From our previous discussion of ν(Au–H) at about 2000 cm^{-1}, it is not easy to relate bands C, D, E and F to H adatoms on Au, these bands might be due to citrate-related species.

4. Conclusions

In this work we have investigated the electrodic behaviour of an acidic citrate $KAu(CN)_2$ bath at a polycrystalline Au cathode by *in situ* confocal Raman spectroscopy. We focussed on the CN^- stretch ν(CN) (at ~2100 cm^{-1}) and Au-adsorbate (~200–600 cm^{-1}) frequency ranges and related them to the electrochemical behaviour. Five kinds of ν(CN) bands were observed as a function of polarization conditions. At high cathodic potentials, well into the hydrogen-evolution range, ν(Au–H) and ν(CN) for the $Au–NC^-$ species dominate. At cathodic polarizations between the $Au/Au(CN)_2^-$ equilibrium potential (~−700 mV) and the potential of inception of hydrogen evolution (~−1200 mV), $Au–NC^-$ species dominate. At slightly anodic potentials the presence of both $Au–NC^-$ and $Au–CN^-$ can be detected and formation of $Au(CN)_2^-$ can be noticed. As the potential grows anodic, adsorbed cyanate can be observed. The peaks related to oxidation products (either of Au: $Au(CN)_2^-$ or of CN^-: OCN^-) do not display a Stark shift, probably because of limited interaction with the Au surface. The other species, which are linked to the external bonding to metallic Au, display a Stark shift whose value can be meant as a diagnostic of the electrodic environment of the CN^- species. The low-frequency range displays a single anodic peak, probably related to OCN^-, the cathodic range is characterised by bands, probably related to Au–N bonding. The fact that several CN^- species are present at the electrode, which form at given potentials and slowly transform into different ones when the potential is varied, might explain the hysteretic and markedly history-dependent cathodic behaviour of CN^--based Au and Au-alloy electrodeposition baths.

References

1. H. Baltruschat and J. Heitbaum, *J. Electroanal. Chem.* **157** (1983) 319.
2. D.S. Corrigan, P. Gao, L.H. Leung and M.J. Weaver, *Langmuir* **2** (1986) 744.
3. P. Gao and M.J. Weaver, *J. Phys. Chem.* **90** (1986) 4057.
4. P. Gao and M.J. Weaver, *J. Phys. Chem.* **93** (1989) 6205.
5. K. Kunimatsu, H. Seki and W.G. Golden, *Chem. Phys. Lett.* **108** (1984) 195.
6. K. Kuminatsu, H. Seki, W.G. Golden, J.G. Gordon and M.R. Philpott, *Surf. Sci.* **158** (1985) 596.
7. K. Kunimatsu, H. Seki, W.G. Golden, J.G. Gordon II and M.R. Philpott, *Langmuir* **4** (1988) 337.
8. M. Tadjeddine and J.P. Flament, *Chem. Phys.* **240** (1999) 39.
9. M. Fleischmann, I.R. Hill and M.E. Pemble, *J. Electroanal. Chem.* **136** (1982) 361.
10. B.M. Chadwick and S.G. Frankiss, *J. Mol. Struct.* **31** (1976) 1.
11. B. Reents and W. Plieth., *in* W.J. Lorenz, W. Plieth (Eds) 'Electrochemical Nanotechnology' (Wiley–VCH, Weinheim, 1998), p. 227.
12. W. Plieth, *Electrochim. Acta* **37** (1992) 2115.
13. F. Texier VII, L. Servant, J.L. Bruneel and F. Argoul, *J. Electroanal. Chem.* **446** (1998) 189.
14. M. Fleischmann, G. Sundholm and Z.Q. Tian, *Electrochim. Acta* **31** (1986) 907.
15. R.L. Birke, T. Lu and J.R. Lombardi, *in* R. Sarma and J.R. Selman (Eds), 'Techniques for Characterization of Electrodes and Electrochemical Processes' (J. Wiley & Sons, New York 1991), pp. 229–230.
16. V.B. Paulissen and C. Korzeniewski, *J. Phys. Chem.* **96** (1992) 4563.
17. A. Tadjeddine, A. Peremans, A. La Rille, W.X. Zheng, M. Tadjeddine and J-P. Flament, *J. Chem. Soc., Faraday Trans.* **92** (1996) 3823.
18. B. Miller and S. Menezes Affonso, *J. Electrochem. Soc.* **123** (1976) 1006.
19. B. Bozzini and P.L. Cavallotti and G. Giovannelli, *in* D. Landolt, M. Matlosz and Y. Sato (Eds), 'Fundamentals of Electrochemical Deposition and Dissolution: 1999' Electrochemical Society Proceedings, Pennington, NJ (1999) PV 99–33, p. 91.
20. J.D.E. McIntyre and W.F. Peck Jr, *J. Electrochem. Soc.* **123** (1976) 1800.
21. B. Ren, X-Q. Li, D.Y. Wu, J-L. Yao, Y. Xie and Z-Q. Tian, *Chem. Phys. Lett.* **322** (2000) 561.
22. P. Guyot-Sionnest and A. Tajeddine, *Chem. Phys. Lett.* **172** (1990) 341.
23. B. Bozzini, G. Giovanelli, C. Lenardi, M. Serra and M. Placidi, 'Effects of organic additives on morphological evolution of electrodeposited Au and Au alloys, *in* Proceedings of the 199th Electrochemical Society Meeting, Washington DC 25–30 March (2001).
24. A.S. Hinman, R.A. Kydd and R.P. Cooney, *J. Chem. Soc., Faraday Trans.* **82** (1986) 3525.
25. Z-Q. Tian, B. Ren, Y-X. Chen, S-Z. Zou and B-W. Mao, *J. Chem. Soc., Faraday Trans.* **92** (1996) 3829.
26. R.J. Nichols and A. Bewick, *J. Electrochem. Soc.* **243** (1988) 445.
27. H. Ogasawa and M. Ito, *Chem. Phys. Lett.* **221** (1994) 213.
28. A. Tadjeddine, A. Peremans and P. Guyot-Sionnest, *Surf. Sci.* **335** (1995) 210.
29. A. Peremans and A. Tadjeddine, *J. Chem. Phys.* **103** (1995) 7197.
30. F. Kitamura, M. Takahashi and M. Ito, *Chem. Phys. Lett.* **130** (1986) 181.